Comparison of Optimal Solutions to Real-Time Path Planning for a Mobile Vehicle

Jian Yang, *Member, IEEE*, Zhihua Qu, *Fellow, IEEE*, Jing Wang, *Member, IEEE*, and Kevin Conrad

***Abstract*—In this paper, we present two near-optimal methods to determine the real-time collision-free path for a mobile vehicle moving in a dynamically changing environment. The proposed designs are based on the polynomial parameterization of feasible trajectories by explicitly taking into account boundary conditions, kinematic constraints, and collision-avoidance criteria. The problems of finding optimal solutions to the parameterized feasible trajectories are then formulated with respect to a near-minimal control-energy performance index and a near-shortest distance performance index, respectively. The obtained optimal solutions are analytical and suitable for practical applications which may require real-time trajectory planning and replanning. Computer simulations are provided to validate the effectiveness of the proposed near-optimal trajectory-planning methods.**

***Index Terms*—Mobile vehicle, moving obstacles, nonholonomic constraints, optimal solution, real-time path planning.**

I. Introduction

DURING the past decades, extensive research efforts have been devoted to plan collision-free paths for mobile vehicles. It is well known that mobile vehicles are generally subject to constraints of rolling without slipping and belong to the so-called nonholonomic systems [15]. Nonholonomy makes path planning much more difficult since the planned paths must take into account both geometric and nonholonomic constraints. In addition, in real applications, it is often the case that we expect to find a collision-free, real-time implementable, and optimal path given the limited sensing range and the dynamically changing operating environment of the mobile vehicle. The main objective of this paper is to present two near-optimal solutions to the trajectory-planning problem of mobile vehicles by explicitly considering kinematic constraints and moving obstacles while making the obtained solutions analytical and real-time implementable.

Manuscript received September 8, 2008; revised May 3, 2009. Date of publication April 1, 2010; date of current version June 16, 2010. This paper was recommended by Associate Editor K. Hirota.

J. Yang was with the Department of Electrical and Computer Engineering, University of Central Florida, Orlando, FL 32816 USA. He is now with Delta Tau Data Systems, Inc., Los Angeles, CA 91311, USA.

Z. Qu is with the Department of Electrical and Computer Engineering, University of Central Florida, Orlando, FL 32816 USA (e-mail: qu@mail.ucf.edu).

J. Wang is with the Computer Engineering Program, Bethune-Cookman University, Daytona Beach, FL 32114 USA (e-mail: wangj@cookman.edu).

K. Conrad was with Lockheed Martin Missiles and Fire Control, Grand Prairie, TX 75051 USA. He is now with Elbit Systems of America, Fort Worth, TX 76179 USA.

Color versions of one or more of the figures in this paper are available online at http://ieeexplore.ieee.org.

Digital Object Identifier 10.1109/TSMCA.2010.2044038

Many techniques have been proposed for the path planning of mobile vehicles. Among them, the potential-field method pioneered in [12] has been widely used, in which the collision-free trajectory is generated along the negative gradient of the defined attractive and repulsive potential-field functions. The subsequent studies can be found in [4], [8], [10], and [23]. In [9], the potential-field method was used in the moving-target tracking problem by planning both the path and the speed of the robot. Nonetheless, the potential-field method is not straightforwardly applicable to mobile vehicles with kinematic constraints since, in the potential-field design, the robot is usually treated as a simple particle. Some approaches have been proposed to modify the generated trajectories from the potential-field method by planning the path into a number of consecutive small segments so as to make each segment locally satisfy the kinematic constraints, such as the online suboptimal obstacle-avoidance algorithm in [20] and the nonholonomic path planner in [13]. The spline method has also been developed in [7], [14], and [17], in which a sequence of splines is used to generate a path through a set of waypoints in the environment. However, prior knowledge of choosing waypoints may not be available due to the fact that the environment is both uncertain and dynamic.

To directly deal with kinematic and geometric constraints, the exhaustive search method was used in [1], where the workspace is divided into multiple regions and a safe path is first established by starting from the initial position and successively searching adjacent regions to the goal. Based on that, the obtained path segments are reconstructed by discretizing the controls and integrating the equations of motion. An alternative method was proposed in [5], in which the obstacle-avoidance criterion and kinematic model are converted into a set of inequality and equality constraints, and numerical iterations are then applied to approximate or determine the path that satisfies all the constraints. There are also some methods addressing the planning problem with moving obstacles. In [11], the dynamic motion planning is decomposed into a static path planning problem and a velocity planning problem. In [6], the time is treated as a state variable and the dynamic motion planning problem is recast as a static one. However, these approaches suffer from the incomplete information, and their solvability is generally not guaranteed. An excellent summary on path planning algorithms for robots can be found in [19]. For sensor-based map building, planning, and navigation of mobile vehicles, a complete description is available in texts [3], [21]. More recently, a new methodology to build compact local maps in real time for outdoor robot navigation was proposed in [2], which is useful for creating a safe trajectory for robot

navigation. On the other hand, for the path planning problem of mobile robots with kinematic constraints, the readers may refer to a recent complete overview given in [16].

In our recent work [18], an analytic solution was presented to determine a collision-free path for a carlike mobile vehicle moving in a dynamically changing environment. Based on the explicit consideration of the kinematic model of the vehicle and the collision-avoidance condition developed for the dynamically changing environment, the family of feasible trajectories and their corresponding steering controls are derived in terms of one adjustable parameter a_6^k. Thus, a class of collision-free path(s) in a closed form is determined. In [18], we simply choose a_6^k with the minimal magnitude to get a specified trajectory from the class. Although this choice generally leads to a feasible trajectory for vehicles, there exist some scenarios in which the planned trajectories may have a big swing with an unnecessary detour which apparently consumes much more control energy to implement. There is no guideline provided in [18] on how to pick a_6^k from the available set in order to yield an optimal trajectory. In [22], a control-energy-related performance index is defined in terms of the inputs of a chained system (a canonical form of the mobile robot); however, the physical meaning of a performance index in terms of the original inputs is hard to interpret.

In this paper, as a natural continuation of the work in [18], we present two analytical solutions to find the near-optimal trajectories for mobile vehicles operating in a dynamically changing environment with moving obstacles by explicitly handling the kinematic constraints and collision avoidance. We define two performance indexes, i.e., one in terms of minimal control energy and the other with respect to the shortest distance. Most importantly, unlike the general nonlinear optimal control problem formulation in which usually the solution can only be found through the time-consuming numerical iteration, the proposed nonlinear optimization problems can be analytically solved while achieving the near-optimal performance due to the utilization of the introduced new performance indexes. The obtained optimal solutions in this paper are computationally efficient and applicable to practical applications which may require real-time trajectory planning and replanning. Computer simulations have validated the effectiveness of the proposed design.

This paper is organized into five sections. In Section II, the admissible trajectories are solved by polynomial parameterization and the feasible trajectories are defined; then, the optimization problem is formulated. In Section III, two optimal performance indexes are defined and the corresponding optimization problems are solved analytically to obtain the real-time implementable trajectories. In Section IV, simulation results that demonstrate the effectiveness of our proposed approaches are presented. A comparison of all mentioned solutions is made, and the advantages of these two near-optimal solutions are illustrated. Section V concludes this paper.

II. Problem Formulation

Consider the trajectory-generation problem for a mobile vehicle moving in a 2-D plane (x–y plane), as shown in Fig. 1.

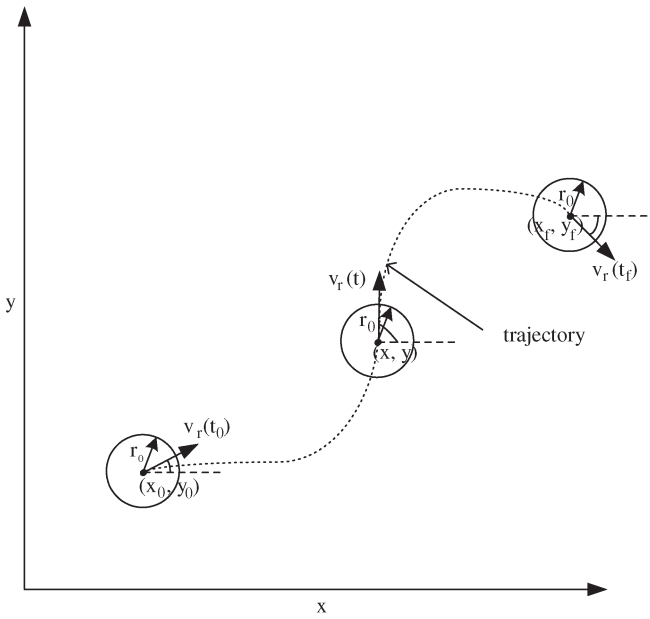

Fig. 1. Mobile vehicle moves from start configuration to end configuration.

The vehicle is represented by a circle with radius r_0. The design objective is to generate an optimal collision-free trajectory for the mobile vehicle moving from the starting point (x_0, y_0) to the ending point (x_f, y_f).

A. Family of Feasible Polynomial Parameterized Trajectories

To find the trajectory from the starting point (x_0, y_0) to the ending point (x_f, y_f), we first define a family of trajectories using polynomial parameterization, i.e., let the family of trajectories be

$$y = [a_0 \quad a_1 \quad \cdots \quad a_p][1 \quad x \quad \cdots \quad x^p]^{\mathrm{T}} \triangleq \vec{a}\vec{x} \qquad (1)$$

where x and y are the coordinates of the vehicle's guidepoint, which is often set to be the center of the circle, and integer $p > 0$. The trajectory-generation problem now becomes to solve for the coefficient vector $\vec{a} \triangleq [a_0 \quad a_1 \quad \cdots \quad a_p]$ using a number of appropriate boundary conditions.

A trajectory is feasible if it satisfies the boundary conditions imposed by kinematic model constraints. In this paper, we assume a set of six initial and terminal conditions in terms of position, orientation, and curvature defined as follows, i.e., the initial conditions are the initial position, orientation, and curvature:

$$(x_0, y_0) \quad \left.\frac{\partial y}{\partial x}\right|_{x=x_0} \quad \left.\frac{\partial^2 y}{\partial x^2}\right|_{x=x_0}. \qquad (2)$$

The terminal conditions are given by the final position, orientation, and curvature as

$$(x_f, y_f) \quad \left.\frac{\partial y}{\partial x}\right|_{x=x_f} \quad \left.\frac{\partial^2 y}{\partial x^2}\right|_{x=x_f}. \qquad (3)$$

Apparently, to make the parameterized trajectory (1) satisfy all six boundary conditions given in (2) and (3), we must

have $p \geq 5$. In particular, the case of $p = 5$ generates a unique solution, while $p > 5$ yields a family of trajectories. In this paper, for ease of calculation, we simply choose $p = 6$. Thus, it follows from (1) that

$$y = \vec{a}\,[1 \quad x \quad x^2 \quad x^3 \quad x^4 \quad x^5 \quad x^6]^{\mathrm{T}} \tag{4}$$

$$\frac{\partial y}{\partial x} = \vec{a}\,[0 \quad 1 \quad 2x \quad 3x^2 \quad 4x^3 \quad 5x^4 \quad 6x^5]^{\mathrm{T}} \tag{5}$$

$$\frac{\partial^2 y}{\partial x^2} = \vec{a}\,[0 \quad 0 \quad 2 \quad 6x \quad 12x^2 \quad 20x^3 \quad 30x^4]^{\mathrm{T}} \tag{6}$$

where $\vec{a} = [a_0 \quad a_1 \quad a_2 \quad a_3 \quad a_4 \quad a_5 \quad a_6]$.

In order to handle the changing environment given the limited sensor range of the vehicle, we further consider the piecewise polynomial parameterized version of (4). Let T be the time for the mobile vehicle to complete its maneuver and T_s be the sampling period such that $\bar{k} = T/T_s$ is an integer. Thus, at the time instant $t_0 + kT_s$, it follows from (4) that we have the piecewise polynomial parameterized trajectory as

$$y = \left[a_0^k \quad a_1^k \quad \cdots \quad a_6^k\right][1 \quad x \quad \cdots \quad x^6]^{\mathrm{T}} \triangleq \vec{a}^k \vec{x}. \tag{7}$$

According to (7), it can be seen that initial conditions keep changing with the motion of the vehicle, i.e., for $k = 0$, we have the same initial conditions as those given in (2), while for other $0 < k < \bar{k}$, the initial conditions become the vehicle's current position, orientation, and curvature at time instant $t_0 + kT_s$, $k = 1, \ldots, \bar{k} - 1$, i.e.,

$$(x_k, y_k) \quad \left.\frac{\partial y}{\partial x}\right|_{x=x_k} \quad \left.\frac{\partial^2 y}{\partial x^2}\right|_{x=x_k}. \tag{8}$$

The terminal conditions are unchanged as given in (3).

To this end, substituting boundary conditions (2), (8), and (3) into (4)–(6) yields

$$\left[a_0^k \quad a_1^k \quad a_2^k \quad a_3^k \quad a_4^k \quad a_5^k\right]^{\mathrm{T}} = (B^k)^{-1}\left(Y^k - A^k a_6^k\right) \tag{9}$$

where

$$Y^k = \begin{bmatrix} y_k \\ \left.\frac{\partial y}{\partial x}\right|_{x=x_k} \\ \left.\frac{\partial^2 y}{\partial x^2}\right|_{x=x_k} \\ y_f \\ \left.\frac{\partial y}{\partial x}\right|_{x=x_f} \\ \left.\frac{\partial^2 y}{\partial x^2}\right|_{x=x_f} \end{bmatrix} \quad A^k = \begin{bmatrix} (x_k)^6 \\ 6(x_k)^5 \\ 30(x_k)^4 \\ (x_f)^6 \\ 6(x_f)^5 \\ 30(x_f)^4 \end{bmatrix}$$

$$B^k = \begin{bmatrix} 1 & x_k & (x_k)^2 & (x_k)^3 & (x_k)^4 & (x_k)^5 \\ 0 & 1 & 2x_k & 3(x_k)^2 & 4(x_k)^3 & 5(x_k)^4 \\ 0 & 0 & 2 & 6x_k & 12(x_k)^2 & 20(x_k)^3 \\ 1 & x_f & (x_f)^2 & (x_f)^3 & (x_f)^4 & (x_f)^5 \\ 0 & 1 & 2x_f & 3(x_f)^2 & 4(x_f)^3 & 5(x_f)^4 \\ 0 & 0 & 2 & 6x_f & 12(x_f)^2 & 20(x_f)^3 \end{bmatrix}.$$

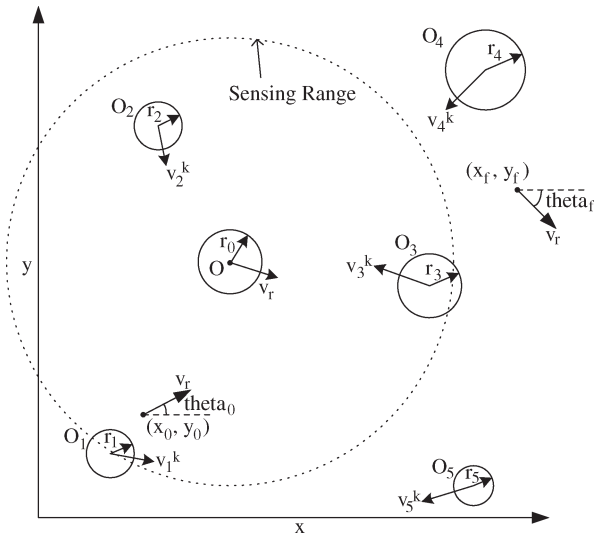

Fig. 2. Mobile vehicle in the presence of moving obstacles with limited sensing range.

It follows from (9) that the family of trajectories in (4) can be further expressed in terms of one adjustable parameter a_6 as

$$y(t) = [1 \quad x \quad x^2 \quad x^3 \quad x^4 \quad x^5](B^k)^{-1} \times \left(Y^k - A^k a_6^k\right) + a_6^k x^6, \qquad t \in [t_0 + kT_s, t_0 + T]. \tag{10}$$

B. Collision-Avoidance Criterion

It is clear that, through the careful choice of a_6^k, we can find a feasible collision-free trajectory from the family of trajectories given in (10) unless the path planning is ill posed (inherently no solution). In what follows, a collision-avoidance criterion for calculating a_6^k is presented [18].

Let us consider the scenario shown in Fig. 2, where a mobile vehicle moves in the presence of circular moving obstacles that are centered at O_i and of radius r_i. For moving objects, the centers of objects O_i are located at (x_i^k, y_i^k) at $t = t_0 + kT_s$, and these objects are all moving with known constant velocities $v_i^k = [v_{i,x}^k, v_{i,y}^k]$ for $t \in [t_0 + kT_s, t_0 + (k+1)T_s)]$, where $k = 0, \ldots, \bar{k} - 1$. The range of the mobile vehicle's sensors is described by a circle centered at $O(t)$ and of radius R_s.

In order to avoid the obstacles, the trajectory have a distance of at least $(r_0 + r_i)$ from the ith obstacle. Then, the collision-avoidance criterion for obstacle O_i in the y–x plane should be as follows: For $x_i' \in [\underline{x}_i', \overline{x}_i']$ with $\underline{x}_i' = x_i^k - r_i - r_0$ and $\overline{x}_i' = x_i^k + r_i + r_0$

$$\left(y_i' - y_i^k\right)^2 + \left(x_i' - x_i^k\right)^2 \geq (r_i + r_0)^2 \tag{11}$$

where $x_i' = x - v_{i,x}^k \tau$, $y_i' = y - v_{i,y}^k \tau$, and $\tau = t - (t_0 + kT_s)$ for $t \in [t_0 + kT_s, t_0 + T]$, with T being the time for the mobile robot to complete its maneuver. Substituting (7) and (9) into (11), the obstacle-avoidance criterion (11) can be further written as

$$\min_{t \in [\underline{t}_i^*, \overline{t}_i^*]} G_i\left(t, \tau, a_6^k\right) = \min_{t \in [\underline{t}_i^*, \overline{t}_i^*]} g_2\left(x(t), k\right)\left(a_6^k\right)^2 + g_{1,i}\left(x(t), k, \tau\right) a_6^k + g_{0,i}\left(x(t), k, \tau\right)|_{\tau = t - t_0 - kT_s} \geq 0 \tag{12}$$

where $[\underline{t}_i^*, \overline{t}_i^*] \subset [t_0 + kT_s, t_f]$ is the time interval (if any) during which $x_i^k \in [x(t) - v_{i,x}^k \tau - r_i - r_0, x(t) - v_{i,x}^k \tau + r_i + r_0]$, and

$$\begin{aligned} g_2(x(t),k) &= \left[(x(t))^6 - \underline{f}(x(t))(B^k)^{-1}A^k\right]^2 \\ g_{1,i}(x(t),k,\tau) &= 2\left[(x(t))^6 - \underline{f}(x(t))(B^k)^{-1}A^k\right] \\ &\quad \times \left[\underline{f}(x(t))(B^k)^{-1}Y^k - y_i^k - v_{i,y}^k\tau\right] \\ g_{0,i}(x(t),k,\tau) &= \left[\underline{f}(x(t))(B^k)^{-1}Y^k - y_i^k - v_{i,y}^k\tau\right]^2 \\ &\quad + \left(x(t) - x_i^k - v_{i,x}^k\tau\right)^2 - (r_i + r_0)^2 \end{aligned}$$

where

$$\underline{f}(x(t)) = \begin{bmatrix} 1 & x & x^2 & x^3 & x^4 & x^5 \end{bmatrix}. \tag{13}$$

It follows that inequality (12) holds if the value of a_6^k lies in the following interval:

$$\Omega_o^k \triangleq \bigcap_{i\in\{1,\ldots,n_o^k\}} \left[(-\infty, \underline{a}_{6,i}^k] \cup [\overline{a}_{6,i}^k, +\infty)\right] \tag{14}$$

where n_o^k is the number of obstacles visible to the vehicle at time instant $t_0 + kT_s$

$$\underline{a}_{6,i}^k = \min_{t\in[\underline{t}_i^*, \overline{t}_i^*]} \frac{-g_{1,i} - \sqrt{(g_{1,i})^2 - 4g_2 g_{0,i}}}{2g_2}$$

$$\overline{a}_{6,i}^k = \min_{t\in[\underline{t}_i^*, \overline{t}_i^*]} \frac{-g_{1,i} + \sqrt{(g_{1,i})^2 - 4g_2 g_{0,i}}}{2g_2}.$$

To this end, it is clear that the class of feasible collision-free trajectories can be analytically solved by selecting $a_6^k \in \Omega_o^k$ [18]. However, no guideline is given for choosing a_6^k to pick the best trajectory within the family. In this paper, we propose two new optimal performance indexes and analytically find the best a_6^k which can yield the near-optimal trajectories in terms of the minimal control energy or the shortest distance.

III. Optimal Solutions for Real-Time Trajectory Planning

A. Energy-Optimal Solution to Trajectory Planning

For a mobile vehicle moving in a 2-D plane, there are generally two control inputs, i.e., the angular velocity of the driving wheel u_1 and the steering velocity u_2. Thus, the energy-optimal control problem can be formulated as follows:

$$\begin{aligned} &\min J_k^{E_1}\left(a_6^k\right) = \int_{t_k}^{t_f} \left(u_1^2 + u_2^2\right) dt \\ &\text{s.t.} \quad \min_{t\in[\underline{t}_i^*, \overline{t}_i^*]} G_i\left(t, \tau, a_6^k\right) \geq 0. \end{aligned} \tag{15}$$

However, since the expressions of u_1 and u_2 in terms of parameterized trajectory (x, y), $(\partial y/\partial x)$, and $(\partial^2 y/\partial x^2)$ are generally nonlinear and complicated (for example, the reader may refer to [18] for the expressions of u_1 and u_2 for the carlike robot), there is no clue on how to analytically solve the optimization problem (15), and we have to use the numerical methods which are time consuming and not a good choice for real-time trajectory planning.

In what follows, we redefine the energy-based performance index and find its analytical solution. For convenience, let the horizontal speed of the vehicle be a constant C, i.e., $\dot{x} = C$. In addition, we can choose the guidepoint of the vehicle such that

$$(\rho u_1)^2 = \dot{x}^2 + \dot{y}^2 \tag{16}$$

where ρ is the radius of the driving wheel. Since the control energy used for steering control u_2 is usually much less, we can omit the steering energy to simplify the performance index in (15) and recast the problem as a near-minimal control-energy optimization problem defined as follows:

$$\begin{aligned} &\min J_k^{E_2}\left(a_6^k\right) = \frac{1}{\rho^2}\int_{t_k}^{t_f} (\dot{x}^2 + \dot{y}^2)\, dt \\ &\text{s.t.} \quad \min_{t\in[\underline{t}_i^*, \overline{t}_i^*]} G_i\left(t, \tau, a_6^k\right) \geq 0. \end{aligned} \tag{17}$$

The following theorem states that an analytical solution to this optimization problem (17) can be obtained.

Theorem 1: Consider the trajectory generation of a mobile vehicle operating in an environment with dynamically moving obstacles. The formulated optimization problem (17) is solvable with

$$\tilde{a}_6^k = \left\{ a_6^k \middle| \min\left|a_6^k - a_6^{k*}\right| \forall\, a_6^k \in \Omega_o^k \right\} \tag{18}$$

where $\tilde{a}_6^k$ is the parameter rendering the feasible collision-free trajectory with the minimal cost $J_k^{E_2}$ and

$$\begin{aligned} a_6^{k*} = &\frac{11\left(\left.\frac{\partial^2 y}{\partial x^2}\right|_{x=x_k} + \left.\frac{\partial^2 y}{\partial x^2}\right|_{x=x_f}\right)}{12(x_k - x_f)^4} \\ &- \frac{22\left(\left.\frac{\partial y}{\partial x}\right|_{x=x_f} - \left.\frac{\partial y}{\partial x}\right|_{x=x_k}\right)}{3(x_f - x_k)^5}. \end{aligned} \tag{19}$$

Proof: We first find the optimal solution without considering the collision-avoidance criteria (12). It follows from (17) and (10) that

$$\begin{aligned} J_k^{E_2}\left(a_6^k\right) &= \frac{1}{\rho^2}\int_{t_k}^{t_f} \left\{ C^2 + \left[C\dot{\underline{f}}(x(t))(B^k)^{-1} \right.\right. \\ &\qquad \left.\left. \times \left(Y^k - A^k a_6^k\right) + 6Ca_6^k x^5\right]^2 \right\} dt \\ &= \frac{C^2}{\rho^2}\int_{t_k}^{t_f} \left[(h_1)^2\left(a_6^k\right)^2 + 2h_1h_2a_6^k + (h_2)^2 + 1\right] dt \\ &= \frac{C^2}{\rho^2}\left[f_1\left(a_6^k\right)^2 + f_2 a_6^k + f_3\right] \end{aligned} \tag{20}$$

where

$$\begin{aligned}\underline{\dot{f}}(x(t)) &= \begin{bmatrix}0 & 1 & 2x & 3x^2 & 4x^3 & 5x^4\end{bmatrix}\\ x(t) &= x_k + C(t-t_k)\\ h_1(t) &= 6x^5 - \underline{\dot{f}}(x(t))\,(B^k)^{-1}A^k\\ h_2(t) &= \underline{\dot{f}}(x(t))\,(B^k)^{-1}Y \qquad (21)\\ f_1 &= \int_{t_k}^{t_f}(h_1)^2\,dt, \quad f_2 = 2\int_{t_k}^{t_f} h_1 h_2\,dt\\ f_3 &= \int_{t_k}^{t_f}\left[(h_2)^2+1\right]dt. \qquad (22)\end{aligned}$$

It follows that $J_k^{E_2}(a_6^k)$ is a second-order polynomial of a_6^k, and its minimal value is achieved when

$$a_6^{k*} = -f_2/(2f_1). \qquad (23)$$

It follows from (22) that

$$\begin{aligned}f_1 &= -\frac{(x_k-x_f)^{10}(t_k-t_f)}{770}\\ f_2 &= \frac{(x_k-x_f)^6(t_k-t_f)\left(\frac{\partial^2 y}{\partial x^2}\Big|_{x=x_k} + \frac{\partial^2 y}{\partial x^2}\Big|_{x=x_f}\right)}{420}\\ &\quad + \frac{2(x_k-x_f)^5(t_k-t_f)\left(\frac{\partial y}{\partial x}\Big|_{x=x_k} - \frac{\partial y}{\partial x}\Big|_{x=x_f}\right)}{105}.\end{aligned}$$

Substituting f_1 and f_2 into (23), we obtain the analytical expression a_6^{k*} in (19).

In the presence of obstacles, the objective is to find the a_6^k that minimizes the cost $J_k^{E_2}$ subject to inequality constraint (12), i.e., we need $a_6^k \in \Omega_o^k$. To this end, by noting the parabola shape of $J_k^{E_2}$ in terms of a_6^k, the optimal value a_6^k that minimizes $J_k^{E_2}$ subject to inequality constraint (12) would be the closest one to a_6^{k*}. Thus, it readily obtains the optimal solution $\tilde{a}_6^k$ in (18). $\diamondsuit$

Remark 1: It is noted that a_6^{k*} is not a function of T, which implies that the optimal solution has nothing to do with the time spent to complete the motion.

Remark 2: The near-minimal control-energy problem is actually an optimization problem with respect to the minimal integration of kinetic energy because the term $(\dot{y}^2+\dot{x}^2)$ stands for the unit kinetic energy of the vehicle. The solution to this problem presents an optimal "total motion" effect to the mobile vehicle.

Remark 3: It follows from (19) that if $(\partial y/\partial x)|_{x=x_k} = (\partial y/\partial x)|_{x=x_f}$ and $(\partial^2 y/\partial x^2)|_{x=x_k} = -(\partial^2 y/\partial x^2)|_{x=x_f}$, we have $a_6^{k*}=0$. Thus, the optimal solution in Theorem 1 reduces to the scheme that we defined to choose a_6^k in our previous paper [18], i.e., we pick a_6^k with the minimal magnitude.

B. Length-Optimal Solution to Trajectory Planning

In this section, we consider finding the length-optimal solution from the family of feasible trajectories. The straightforward strategy to obtain the shortest path is to use the line integration with respect to the arc length, i.e., let the performance index be

$$J_k^{L_1}\left(a_6^k\right) = \int_{x_k}^{x_f}\sqrt{1+\left(\frac{dy}{dx}\right)^2}\,dx. \qquad (24)$$

However, no analytical solution of a_6^k can be solved from (24).

On the other hand, we may consider the following performance index:

$$J_k^{L_2}\left(a_6^k\right) = \int_{x_k}^{x_f}\left|y - \frac{y_f-y_0}{x_f-x_0}(x(t)-x_0) - y_0\right|dx \qquad (25)$$

which represents the area between the generated trajectory and the straight line connecting the starting point and the ending point. However, there is also no analytical solution available to the optimization problem (25). Motivated by the route of the least square used in the linear regression and variance analysis in statics, in this paper, we formulate the performance index as

$$J_k^{L_3}\left(a_6^k\right) = \int_{x_k}^{x_f}\left[y - \frac{y_f-y_0}{x_f-x_0}(x-x_0) - y_0\right]^2 dx. \qquad (26)$$

The performance index is an integration to the square of the vertical coordinate difference between the class of parameterized trajectories and the initial straight line. To this end, the optimal trajectory-generation problem can be formulated as

$$\begin{aligned}\min J_k^{L_3}\left(a_6^k\right) &= \int_{x_k}^{x_f}\left[y - \frac{y_f-y_0}{x_f-x_0}(x-x_0) - y_0\right]^2 dx\\ \text{s.t.} \quad &\min_{t\in\left[\underline{t}_i^*,\overline{t}_i^*\right]} G_i\left(t,\tau,a_6^k\right) \ge 0. \qquad (27)\end{aligned}$$

Similar to the performance index in (25), the performance index in (26) can also make the trajectory stay close to the straight line.

In the following, we present the analytical solution to the optimization problem (27) in Theorem 2.

Theorem 2: Consider the trajectory generation of a mobile vehicle operating in an environment with dynamically moving obstacles. The formulated optimization problem (27) is solvable with

$$\bar{a}_6^k = \left\{a_6^k \middle| \min\left|a_6^k - a_6^{k**}\right| \forall\, a_6^k \in \Omega_o^k\right\} \qquad (28)$$

where $\bar{a}_6^k$ is the parameter rendering the feasible collision-free trajectory with the minimal cost $J_k^{L_3}(a_6^k)$ and

$$\begin{aligned}a_6^{k**} &= \frac{13\left(\frac{\partial^2 y}{\partial x^2}\Big|_{x=x_k} + \frac{\partial^2 y}{\partial x^2}\Big|_{x=x_f}\right)}{12(x_k-x_f)^4}\\ &\quad + \frac{117\left(\frac{\partial y}{\partial x}\Big|_{x=x_f} - \frac{\partial y}{\partial x}\Big|_{x=x_k}\right)}{10(x_k-x_f)^5}\\ &\quad + \frac{429\left[\frac{y_f-y_0}{x_f-x_0}(x_k-x_f) - (y_k-y_f)\right]}{10(x_k-x_f)^6}. \qquad (29)\end{aligned}$$

Proof: We first find the optimal solution without considering the collision-avoidance criteria (12). It follows from (26) and (10) that

$$\begin{aligned} J_k^{L_3}\left(a_6^k\right) &= \int_{x_k}^{x_f} \left[\underline{f}\left(x(t)\right)\left(B^k\right)^{-1}\left(Y^k - A^k a_6^k\right) + a_6^k x^6 \right. \\ &\qquad \left. - (y_f - y_0)(x - x_0)/(x_f - x_0) - y_0\right]^2 dx \\ &= C\int_{t_k}^{t_f} \left[(m_1)^2\left(a_6^k\right)^2 + 2m_1 m_2 a_6^k + (m_2)^2\right] dt \\ &= C\left[n_1\left(a_6^k\right)^2 + n_2 a_6^k + n_3\right] \end{aligned} \tag{30}$$

where

$$\begin{aligned} m_1(t) &= x^6 - \underline{f}\left(x(t)\right)\left(B^k\right)^{-1}A^k \\ m_2(t) &= \underline{f}\left(x(t)\right)\left(B^k\right)^{-1}Y - \frac{y_f - y_0}{x_f - x_0}(x - x_0) - y_0 \\ n_1 &= \int_{t_k}^{t_f} (m_1)^2\, dt, \quad n_2 = 2\int_{t_k}^{t_f} m_1 m_2\, dt \\ n_3 &= \int_{t_k}^{t_f} (m_2)^2\, dt. \end{aligned} \tag{31}$$

It follows that $J_k^{L_3}(a_6^k)$ is a second-order polynomial of a_6^k, and its minimal value is achieved when

$$a_6^{k**} = -n_2/(2n_1). \tag{32}$$

It follows from (31) that

$$\begin{aligned} n_1 &= -\frac{(x_k - x_f)^{12}(t_f - t_k)}{12012} \\ n_2 &= \frac{(x_k - x_f)^6(t_f - t_k)}{27720} \\ &\quad \times \left[5\left(\left.\frac{\partial^2 y}{\partial x^2}\right|_{x=x_k} + \left.\frac{\partial^2 y}{\partial x^2}\right|_{x=x_f}\right)(x_k - x_f)^2 \right. \\ &\qquad + 54\left(\left.\frac{\partial y}{\partial x}\right|_{x=x_f} - \left.\frac{\partial y}{\partial x}\right|_{x=x_k}\right)(x_k - x_f) \\ &\qquad \left. + 198\frac{(y_f - y_0)(x_k - x_f) - (y_k - y_f)(x_f - x_0)}{x_f - x_0}\right]. \end{aligned} \tag{33}$$

Substituting n_1 and n_2 into (32) yields the analytical expression a_6^{k**} in (29). In the presence of obstacles, following the similar argument in Theorem 1, we can obtain the optimal solution $\bar{a}_6^k$ as that in (28). ♢

Remark 4: It is of interest to note that if the performance index in (24) is changed to

$$J_k^{\circ}\left(a_6^k\right) = \int_{x_k}^{x_f}\left[1 + \left(\frac{dy}{dx}\right)^2\right] dx \tag{34}$$

we can also find an optimal analytic solution of a_6^k. However, the minimization of (34) does not imply the minimization of (24) with the minimal length. It cannot guarantee that the trajectories stay as close as possible to the initial straight line either. In this sense, the performance index given in (26) is the best choice which gives the analytical near-shortest solution. In addition, an interesting result can be observed by considering the case of $\dot{x} = C$. It follows that

$$\begin{aligned} J_k^{\circ}\left(a_6^k\right) &= \int_{x_k}^{x_f}\left[1 + \left(\frac{dy}{dx}\right)^2\right] dx = C\int_{t_k}^{t_f}\left[1 + \left(\frac{dy}{dx}\right)^2\right] dt \\ &= C\int_{t_k}^{t_f}\left[1 + \left(\frac{\dot{y}}{\dot{x}}\right)^2\right] dt = C\int_{t_k}^{t_f}\left[1 + \left(\frac{\dot{y}}{C}\right)^2\right] dt \\ &= \frac{1}{C}\int_{t_k}^{t_f}(\dot{x}^2 + \dot{y}^2)\, dt \end{aligned} \tag{35}$$

which shows that the solution from the performance index $J_k^{\circ}(a_6^k)$ is the same as that we obtained with the near-minimal control-energy method.

Remark 5: In the performance index (26), we can dynamically update the reference straight line connecting the starting and the ending point, i.e., we redefine the performance index as

$$J_k^{L_4}\left(a_6^k\right) = C\int_{t_k}^{t_f}\left[y - K_k\left(x(t) - x_k\right) - y_k\right]^2 dt \tag{36}$$

where

$$K_k = (y_f - y_k)/(x_f - x_k).$$

Although tedious, it can be computed that the optimal solution of a_6^k for minimizing $J_k^{L_4}(a_6^k)$ without obstacles is

$$\begin{aligned} a_6^{k***} &= \frac{13\left(\left.\frac{\partial^2 y}{\partial x^2}\right|_{x=x_k} + \left.\frac{\partial^2 y}{\partial x^2}\right|_{x=x_f}\right)}{12(x_k - x_f)^4} \\ &\quad + \frac{117\left(\left.\frac{\partial y}{\partial x}\right|_{x=x_f} - \left.\frac{\partial y}{\partial x}\right|_{x=x_k}\right)}{10(x_k - x_f)^5}. \end{aligned} \tag{37}$$

In the presence of an obstacle, the optimal a_6^k can be found by $\min|a_6^k - a_6^{k***}|$ and $a_6^k \in \Omega_o^k$.

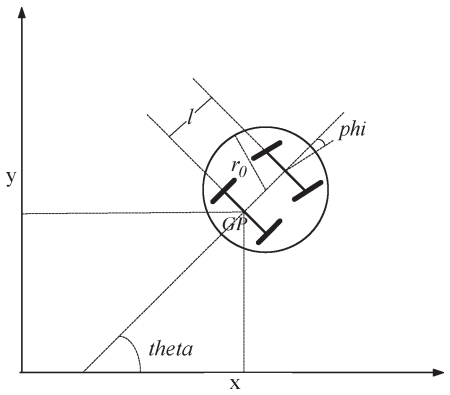

Fig. 3. Carlike vehicle.

IV. Simulation

To illustrate the effectiveness of the proposed optimal solutions, we apply them to the trajectory-generation problem of the carlike mobile vehicle.

A. Model of Carlike Mobile Vehicle

A carlike vehicle is shown in Fig. 3; its front wheels are steering wheels, and its rear wheels are driving wheels but have a fixed orientation. The distance between the two wheel–axle centers is l, and the whole vehicle is physically within a circle of radius r_0 and centered at the midpoint along the line connecting the two axle centers. Let the guidepoint (GP) be set as the midpoint of the rear wheel–axle. The model of the mobile vehicle can be obtained as

$$\begin{pmatrix} \dot{x} \\ \dot{y} \\ \dot{\theta} \\ \dot{\phi} \end{pmatrix} = \begin{pmatrix} \rho\cos(\theta) & 0 \\ \rho\sin(\theta) & 0 \\ \frac{\rho}{l}\tan(\phi) & 0 \\ 0 & 1 \end{pmatrix} \begin{pmatrix} u_1 \\ u_2 \end{pmatrix} \tag{38}$$

where (x, y) are the Cartesian coordinates of the guidepoint, θ is the orientation of the car body with respect to the x axis, ϕ is the steering angle, ρ is the driving wheel radius, u_1 is the angular velocity of the driving wheel, and u_2 is the steering rate. The range of ϕ is limited within $(-\pi/2, \pi/2)$ in practice due to control singularity. Define $q = [x, y, \theta, \phi]$; the trajectory-generation problem is to make the vehicle move from the initial configuration $q^0 = [x_0, y_0, \theta_0, \phi_0]$ to the final configuration $q^f = [x_f, y_f, \theta_f, \phi_f]$ in time T.

It follows from (38) that

$$\frac{\partial y}{\partial x} = \tan(\theta) \quad \frac{\partial^2 y}{\partial x^2} = \frac{\tan(\phi)}{l\cos^3(\theta)}. \tag{39}$$

From (39), it is obvious that θ and ϕ can be expressed in terms of $\partial y/\partial x$ and $\partial^2 y/\partial x^2$; therefore, the polynomial parameterization will match the kinematic model of the carlike mobile vehicle. Moreover, the boundary conditions are

$$\begin{aligned} (x_0, y_0) \quad & \left.\frac{\partial y}{\partial x}\right|_{x=x_0} = \tan(\theta_0) \quad \left.\frac{\partial^2 y}{\partial x^2}\right|_{x=x_0} = \frac{\tan(\phi_0)}{l\cos^3(\theta_0)} \\ (x_f, y_f) \quad & \left.\frac{\partial y}{\partial x}\right|_{x=x_f} = \tan(\theta_f) \quad \left.\frac{\partial^2 y}{\partial x^2}\right|_{x=x_f} = \frac{\tan(\phi_f)}{l\cos^3(\theta_f)}. \end{aligned} \tag{40}$$

Now, let us consider the collision-avoidance criteria for the carlike mobile vehicle. Note that the coordinate of the center of the carlike vehicle is $(x + (l/2)\cos(\theta), y + (l/2)\sin(\theta))$. Thus, the collision-avoidance criterion (11) becomes

$$\left(y + \frac{l}{2}\sin(\theta) - y_i^k - v_{i,y}^k\tau\right)^2 + \left(x + \frac{l}{2}\cos(\theta) - x_i^k - v_{i,x}^k\tau\right)^2 \geq (r_i + r_0)^2. \tag{41}$$

By repeating the exactly same derivation in our previous paper [18], we can obtain the same inequalities, as shown in (12) with $x_i^k \in [x(t) - v_{i,x}^k\tau - r_i - r_0, x(t) - v_{i,x}^k\tau + 0.5l + r_i + r_0]$ and $g_{0,i}(x(t), k, \tau) = [\underline{f}(x(t))(B^k)^{-1}Y^k - y_i^k - v_{i,y}^k\tau]^2 + (x(t) - x_i^k - v_{i,x}^k\tau)^2 - (r_i + r_0 + 0.5l)^2$.

In addition, once a_6^k is obtained, we can find the following control inputs u_1 and u_2, as shown in [18]:

$$\begin{aligned} u_1 &= \frac{w_1}{\rho\cos(\theta)} \\ u_2 &= -\frac{3\sin(\theta)}{l\cos^2(\theta)}\sin^2(\phi)w_1 + l\cos^3(\theta)\cos^2(\phi)w_2 \end{aligned} \tag{42}$$

where

$$\begin{aligned} w_1 &= \frac{x_f - x_0}{T} = C \\ w_2 &= 6\left[a_3^k + 4a_4^k x_1^k + 10a_5^k\left(x_1^k\right)^2 + 20a_6^k\left(x_1^k\right)^3\right]w_1 \\ &\quad + 24\left[a_4^k + 5a_5^k x_1^k + 15a_6^k\left(x_1^k\right)^2\right](t - t_0 - kT_s){w_1}^2 \\ &\quad + 60\left(a_5^k + 6a_6^k x_1^k\right)(t - t_0 - kT_s)^2{w_1}^3 \\ &\quad + 120a_6^k(t - t_0 - kT_s)^3{w_1}^4. \end{aligned} \tag{43}$$

In next section, we present the simulation results for the optimal solution results obtained in Theorems 1 and 2. It is worth mentioning that the proposed optimal methods are also applicable to address other mobile vehicles, such as a differential-driven vehicle.

B. Trajectory Comparison Without Obstacles

In the simulation, we first consider the case without obstacles and then the case with moving obstacles. We use the following settings for the vehicle:

1) Vehicle parameters: $r = 1$, $l = 0.8$, and $\rho = 0.2$.
2) Boundary conditions: $q^0 = (0, 0, (\pi/4), 0)$ and $q^f = (17, 10, -(\pi/4), 0)$, where $t_0 = 0$ and $T = 40$ s.

In the following figures, the scales are same and all quantities conform to a given unit system, for instance, meters, meters per second, etc.

For the case without obstacles, as shown in Table I, we obtain seven different trajectories with the different choices of a_6^k. Among them, path 1 corresponds to the shortest distance using performance index $J_k^{L_1}(a_6^k)$ in (24); path 2 is for $J_k^{L_3}(a_6^k)$ in (26); path 3 is for simply making $a_6^k = 0$; path 4 is for $J_k^{L_2}(a_6^k)$ in (25); path 5 is for $J_k^{E_2}(a_6^k)$ in (17); path 6 is for $J_k^{E_1}(a_6^k)$ in (15); and path 7 is for the method in [22]. Paths 1, 4, 6, and 7 are obtained by numerical nonlinear programming. The

TABLE I
PATH COMPARISON WITHOUT OBSTACLES

	Path 1 Shortest	Path 2 Near shortest	Path 3 $a_6^k = 0$	Path 4 Smallest area	Path 5 Near-minimal control energy	Path 6 Minimal control energy	Path 7 Minimal control energy(chained form)
Length	21.97	22.28	23.62	22.07	21.98	21.98	23.62
Energy	1235.2	1301.8	1431.4	1261.4	1230.2	1230.2	1431.4
$a_6 \times (10^{-5})$	1.21	1.65	0	1.44	1.08	1.08	0

TABLE II
PATH COMPARISON WITH OBSTACLES

	Shortest	Near shortest	Minimal $\lvert a_6^k \rvert$	Smallest area	Near-minimal control energy	Minimal control energy	Minimal control energy(chained form)
Length	22.43	22.75	36.78	22.64	22.75	22.46	33.39
Energy	1291.5	1334.1	3558.0	1312.1	1334.1	1284.8	2975.4

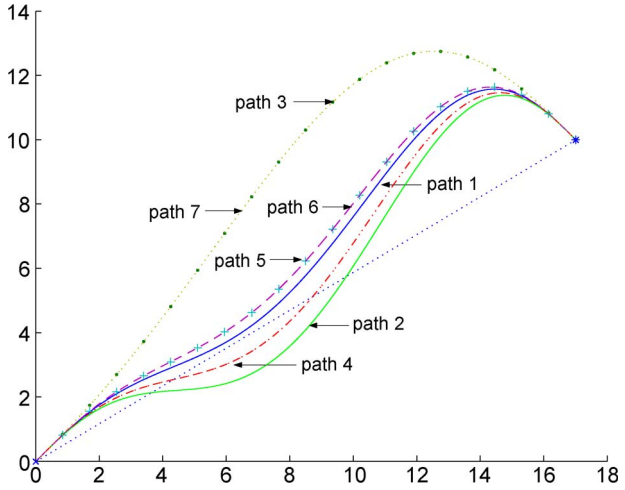

Fig. 4. Path comparison without obstacles.

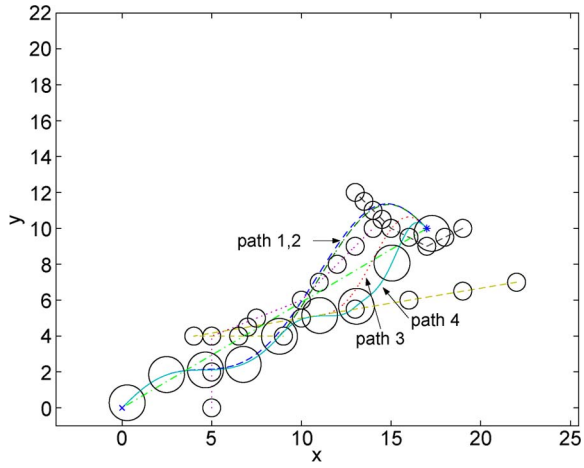

Fig. 5. Shortest path of the vehicle and paths of obstacles.

trajectories are shown in Fig. 4, where the x-mark represents the starting position and the star denotes the ending position. The length of the paths, the corresponding control energy, and the selected value of a_6^k are shown in Table I. It should be noted that, for comparison purposes, while a_6^k in Tables I and II are obtained either numerically or analytically for different methods, the length and control-energy values in both tables are computed based on the same set of equations, i.e., (24) and (15), respectively.

This result verifies that the proposed near-minimal energy-optimal method (path 5) reduces the control energy effectively. More than 14% of control energy is saved by the optimal technique compared with that of path 3 which is the method used in [18] for the obstacle-free case. The shortest path is path 1, while the proposed near-shortest method (path 2) makes the trajectory stay as close as possible to the initial straight line, and its length is only 2% longer than that of path 1. In comparison, although paths 2 and 5 are only near-optimal, their values of a_6^k can be computed analytically based on the solutions provided in Theorems 1 and 2, while the solutions for paths 1, 4, and 6 have to be calculated offline numerically. In the presence of moving obstacles, the methods generating paths 2 and 5 would be good choices for real-time implementation.

Remark 6: It is noted that the length of the path obtained by the near-minimal control-energy method is shorter than the one by the near-shortest method. The near-minimal control-energy problem minimized the L^2 norm of the speed; hence, the norm of the speed is minimized on a certain level. Furthermore, since the time T for the vehicle to finish all the maneuvers is fixed, as a by-product, the length of the path is minimized to a certain extent by the near-minimal control-energy methodology. However, it should be pointed out that the near-minimal energy performance index (17) is close to the energy index in (15) and that the near-shortest path performance index (27) is close to the length index in (24). Therefore, for general cases, there is no reason to claim that the path obtained by the near-optimal control-energy method would be shorter than that by the near-shortest method.

C. Trajectory Comparison With Moving Obstacle

We consider the following settings for the case with moving obstacles:

1) Moving obstacles: $n_0 = 3$, $O_1(t_0) = [5, 0]^{\mathrm{T}}$, $O_2(t_0) = [9, 4]^{\mathrm{T}}$, $O_3(t_0) = [19, 10]^{\mathrm{T}}$, and $r_i = 0.5$ for $i = 1, 2, 3$.
2) Speeds of obstacles:

$$v_1^0 = [0, 0.4]^{\mathrm{T}} \quad v_1^1 = [0.5, 0.2]^{\mathrm{T}} \quad v_1^2 = v_1^3 = [0.2, 0.2]^{\mathrm{T}}$$
$$v_2^0 = [-0.5, 0]^{\mathrm{T}} \quad v_2^1 = [0.6, 0.1]^{\mathrm{T}} \quad v_2^2 = v_2^3 = [0.6, 0.1]^{\mathrm{T}}$$
$$v_3^0 = [-0.2, -0.1]^{\mathrm{T}} \quad v_3^1 = [-0.2, 0.1]^{\mathrm{T}}$$
$$v_3^2 = v_3^3 = [-0.1, 0.1]^{\mathrm{T}}.$$

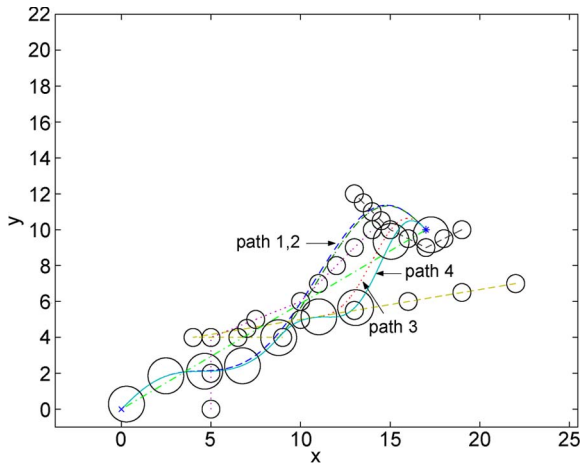

Fig. 6. Near-shortest path of the vehicle and paths of obstacles.

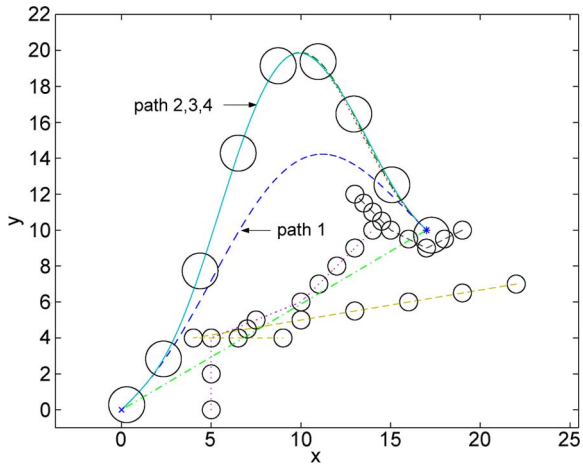

Fig. 7. Path of the vehicle with minimal $|a_6^k|$ and paths of obstacles.

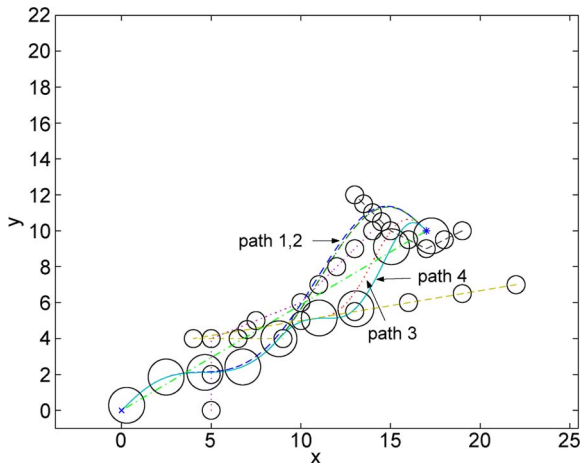

Fig. 8. Path of the vehicle with the smallest area and paths of obstacles.

The sampling period is adaptively chosen according to the speed changes detected, and hence, $T_s = 10$ s.

3) The sensor range $R_s = 7$ implies that the vehicle has a limited sensor range; thus, the vehicle detects the presence of objects 1, 2, and 3 intermittently.

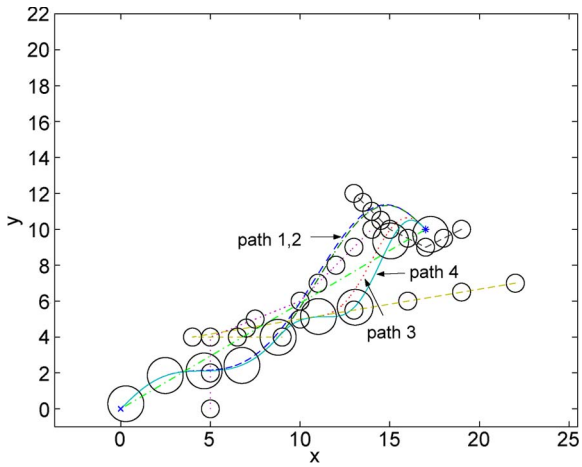

Fig. 9. Path of the vehicle with near-minimal control energy and paths of obstacles.

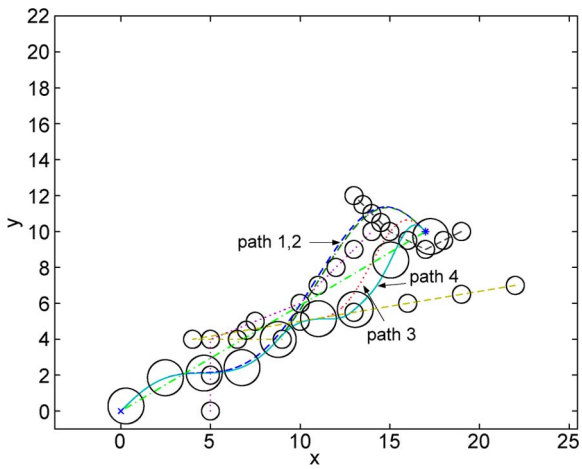

Fig. 10. Path of the vehicle with minimal control energy and paths of obstacles.

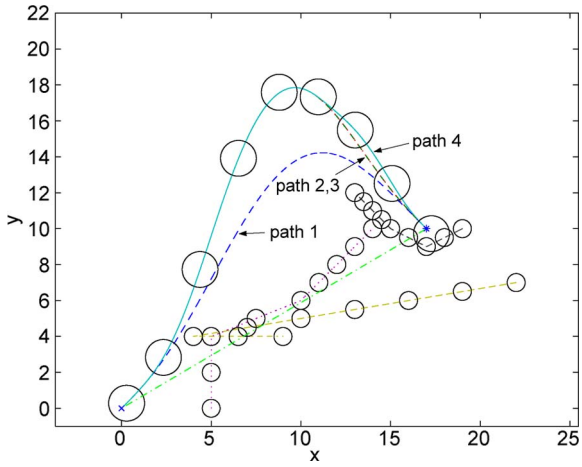

Fig. 11. Path of the vehicle with minimal control energy in chained form and paths of obstacles.

The simulation results are shown in Figs. 5–11. The position of the vehicle is marked by a big circle, and the positions of the three objects are marked by small circles which are drawn every 5 s.

Fig. 5 shows the results for the shortest distance method using performance index $J_k^{L_1}(a_6^k)$ in (24), Fig. 6 is for $J_k^{L_3}(a_6^k)$ in (26), Fig. 7 corresponds to the choice of an a_6^k of minimal magnitude, Fig. 8 is for $J_k^{L_2}(a_6^k)$ in (25), Fig. 9 is for $J_k^{E_2}(a_6^k)$ in (17), Fig. 10 is for $J_k^{E_1}(a_6^k)$ in (15), and Fig. 11 is for the method in [22].

In all figures, path 1 is the trajectory solution if the objects would maintain their velocities at v_i^0 for $t = [0, 40]$, path 2 is the trajectory if the object velocities would be kept at v_i^1 for $t = [10, 40]$, path 3 is the trajectory if the object velocities would be kept at v_i^2 for $t = [20, 40]$, and path 4 is the complete solution of the entire trajectory by considering all the speed changes of all objects. The results about path 4 obtained from different methods are shown in Table II. The paths of obstacles 1–3 are represented by the dotted, dashed–dotted, and dashed lines, respectively.

As shown in Figs. 7 and 11 and Table II, it is found that the trajectories generated by a_6^k using our previous methods in [18] and [22] contain a longer swing and consume much more control energy than what the trajectory got from our proposed optimal methods. The near-minimal control-energy solution (Fig. 9) reduces the consumed energy to 44.8% of the one that applied the minimal control energy in chained form. The near-shortest method (Fig. 6) reduces 38.2% of length when compared with the path generated by choosing a minimal $|a_6^k|$. Most importantly, for the results in Figs. 9 and 6, the values of a_6^k at each sampling time instant are computed online using the solutions provided in Theorems 1 and 2.

V. Conclusion

In this paper, two real-time implementable near-optimal solutions to the trajectory-generation problem of mobile vehicles moving in a dynamic environment with moving obstacles have been presented. Based on a piecewise polynomial parameterization of all feasible trajectories, the trajectory-generation problem is formulated as a constrained parameter optimization problem subject to the boundary conditions of the system and the inequality constraints imposed by the obstacle-avoidance criterion. Different performance indexes are defined to obtain optimal solutions. Compared with other optimal criteria, the proposed near-shortest and near-minimal control-energy performance indexes achieve the near-optimal performance in terms of the reduced control energy and path length, while their solutions are analytical and suitable for real-time trajectory planning. The proposed framework is applied to a carlike mobile vehicle, and simulation results have verified the effectiveness of the proposed methods.

References

[1] J. Barraquand and J.-C. Latombe, "Nonholonomic multibody mobile robots: Controllability and motion planning in the presence of obstacles," in *Proc. IEEE Int. Conf. Robot. Autom.*, Sacramento, CA, Apr. 1991, pp. 2328–2335.

[2] C. Castejon, D. Blanco, and L. Moreno, "Compact modeling technique for outdoor navigation," *IEEE Trans. Syst., Man, Cybern. A, Syst., Humans*, vol. 38, no. 1, pp. 9–24, Jan. 2008.

[3] H. Choset, K. M. Lynch, S. Hutchinson, G. Kantor, W. Burgard, L. E. Kavraki, and S. Thrun, *Principles of Robot Motion: Theory, Algorithms, and Implementations*. Cambridge, MA: MIT Press, 2005.

[4] J.-H. Chuang, "Potential-based modeling of three-dimensional workspace for obstacle avoidance," *IEEE Trans. Robot. Autom.*, vol. 14, no. 5, pp. 778–785, Oct. 1998.

[5] A. W. Divelbiss and J. T. Wen, "A path space approach to nonholonomic motion planning in the presence of obstacles," *IEEE Trans. Robot. Autom.*, vol. 13, no. 3, pp. 443–451, Jun. 1997.

[6] M. Erdmann and T. Lozano-Perez, "On multiple moving objects," in *Proc. IEEE Int. Conf. Robot. Autom.*, San Francisco, CA, Apr. 1986, pp. 1419–1424.

[7] J. Evans, H. Eren, and C. C. Fung, "Implementation of the spline method for mobile robot path control," in *Proc. 16th IEEE IMTC*, May 1999, vol. 2, pp. 739–744.

[8] S. S. Ge and Y. J. Cui, "New potential functions for mobile robot path planning," *IEEE Trans. Robot. Autom.*, vol. 16, no. 5, pp. 615–620, Oct. 2000.

[9] L. Huang, "A potential field approach for controlling a mobile robot to track a moving target," in *Proc. 22nd IEEE Int. Symp. Intell. Control*, Singapore, Oct. 2007, pp. 66–70.

[10] Y. K. Hwang and N. Ahuja, "A potential field approach to path planning," *IEEE Trans. Robot. Autom.*, vol. 8, no. 1, pp. 23–32, Feb. 1992.

[11] K. Kant and S. W. Zucker, "Planning collision free trajectories in time-varying environments: A two level hierarchy," in *Proc. IEEE Int. Conf. Robot. Autom.*, Raleigh, NC, 1988, pp. 1644–1649.

[12] O. Khatib, "Real-time obstacle avoidance for manipulator and mobile robots," *Int. J. Robot. Res.*, vol. 5, no. 1, pp. 90–98, 1986.

[13] J.-P. Laumond, P. E. Jacobs, M. Taix, and R. M. Murray, "A motion planner for nonholonomic mobile robots," *IEEE Trans. Robot. Autom.*, vol. 10, no. 5, pp. 577–593, Oct. 1994.

[14] A. Gardel and J. L. Lazaro, "Adaptive workspace modeling, using regression methods, and path planning to the alternative guide of mobile robots in environments with obstacles," in *Proc.7th IEEE ETFA*, Oct. 1999, vol. 1, pp. 529–534.

[15] Z. X. Li and J. Canny, *Nonholonomic Motion Planning*. Dordrecht, The Netherlands: Kluwer, 1992.

[16] J. Minguez, F. Lamiraux, and J.-P. Laumond, "Motion planning and obstacle avoidance," in *Handbook of Robotics*, B. Siciliano and O. Khatib, Eds. New York: Springer-Verlag, 2008, pp. 827–852.

[17] M. Bertozzi, A. Fascioli, A. Broggi, A. Piazzi, and C. G. Lo Bianco, "Quintic g2-splines for the iterative steering of vision-based autonomous vehicles," *IEEE Trans. Intell. Transp. Syst.*, vol. 3, no. 1, pp. 27–36, Mar. 2002.

[18] Z. Qu, J. Wang, and C. E. Plaisted, "A new analytical solution to mobile robot trajectory generation in the presence of moving obstacles," *IEEE Trans. Robot.*, vol. 20, no. 6, pp. 978–993, Dec. 2004.

[19] S. M. LaValle, *Planning Algorithms*. New York: Cambridge Univ. Press, 2006.

[20] S. Sundar and Z. Shiller, "Optimal obstacle avoidance based on the Hamilton–Jacobi–Bellman equation," *IEEE Trans. Robot. Autom.*, vol. 13, no. 2, pp. 305–310, Apr. 1997.

[21] S. Thrun, W. Burgard, and D. Fox, *Probabilistic Robotics*. Cambridge, MA: MIT Press, 2005.

[22] J. Wang, J. Yang, and Z. Qu, "An optimal solution to mobile robot trajectory generation in the presence of moving obstacles," in *Proc. 10th Int. Meeting Robot. Remote Syst.*, Gainesville, FL, Mar. 2004.

[23] C. W. Warren, "A technique for autonomous underwater vehicle route planning," *IEEE Trans. Ocean. Eng.*, vol. 15, no. 3, pp. 199–204, Jul. 1990.

Jian Yang (M'09) received the Ph.D. degree in electrical engineering from the University of Central Florida, Orlando, in 2008.

Since August 2007, he has been with Delta Tau Data Systems, Inc., Los Angeles, CA, as an Electrical Engineer. His current research interests include control application, motion planning, and power electronics.

Zhihua Qu (M'90–SM'93–F'10) received the Ph.D. degree in electrical engineering from the Georgia Institute of Technology, Atlanta, in 1990.

Since then, he has been with the University of Central Florida, Orlando, where he is currently a Professor with the Department of Electrical and Computer Engineering. He has published a number of papers in these areas and is the author of three books, *Robust Control of Nonlinear Uncertain Systems* (Wiley Interscience, 1998), *Robust Tracking Control of Robotic Manipulators* (IEEE Press, 1996), and *Cooperative Control of Dynamical System* (Springer-Verlag, 2009). He is currently an Associate Editor of *Automatica* and the *International Journal of Robotics and Automation*. His main research interests are nonlinear and networked systems, cooperative and robust controls, robotics and autonomous vehicle systems, and energy systems.

Dr. Qu is an Associate Editor for the IEEE TRANSACTIONS ON AUTOMATIC CONTROL and also serves on the Board of Governors for the IEEE Computer Science Society.

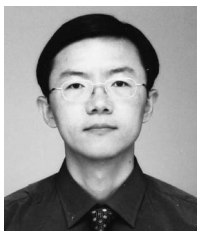

Jing Wang (M'01) received the Ph.D. degree in control theory and control engineering from Central South University, Changsha, China, in 1997.

He was a Postdoctoral Research Fellow with the Institute of Computing Technology, Chinese Academy of Sciences, Beijing, China, from 1997 to 1999, and with the National University of Singapore, Singapore, from 1999 to 2002. From 2002 to 2007, he was with the School of Electrical and Computer Science, University of Central Florida, Orlando, as a Research Assistant Professor. Since 2007, he has been an Assistant Professor in computer science and computer engineering with Bethune-Cookman University, Daytona Beach, FL. His main research interests include autonomous robotics, cooperative control, nonlinear control, sensor networks, and control applications.

Kevin Conrad received the B.S.M.E. degree from Rice University, Houston, TX, and the M.S.M.E. degree from The University of Texas at Arlington, in 1998 and 1999, respectively.

He is currently the Advanced Systems Program Manager for Land Solutions at Elbit Systems of America (ESA), Fort Worth, TX. His responsibilities include oversight of ESA's remote weapon stations programs, CREW product line, as well as unmanned systems development projects. Prior to joining the ESA team, he was the Research and Development Manager for the UGV group at Lockheed Martin Missiles and Fire Control, Dallas, TX, specializing in robotic vehicle design, human–robotic interface, dynamic controls, localization, terrain and situational perception, sensor and data fusion, artificial intelligence, and systems integration. Other roles and responsibilities include Program Manager of the DARPA Unmanned Ground Combat Vehicle program, the predecessor to the ARV-A(L), and Principal Investigator on several collaborative IR&D projects.